Techno-economic analysis of an off-grid hybrid energy system with a new multiyear load growth optimisation technique in HOMER.

Temitope Roland Alademehin (Researcher), **Jonathan Swingler** (Supervisor*).*

For the degree in MSc Renewable Energy Engineering School of Engineering and Physical Sciences, Heriot-Watt University, Edinburgh, UK

ARTICLE INFO

Submitted: 23/08/2019

Keywords:

Hybrid Energy System (HES)

Techno-Economic

Multiyear load growth (MYLG)

HOMER

Desalination

Sensitivity analysis

ABSTRACT

The inaccessibility of affordable electricity and clean water has impaired the socio-economic and health conditions of the people in remote areas. This study explored the multiyear load growth effect and techno-economic feasibility for the implementation of cost-effective hybrid energy systems (HESs) to serve the growing electricity and water desalination requirement of an off-grid rural community in Nigeria coupled with a unique optimisation technique. Three different design scenarios based on the number of hydrokinetic turbine(s) (HK1, HK2 & HK3) were simulated in Hybrid Optimisation of Multiple Energy Resources (HOMER) to obtain the optimum configuration of the HESs, required to meet the growing demand for an increasing peak power of 84 kW - 175 kW in 25 years. To avoid high discrepancy between MYLG and non-MYLG results, a novel pre-optimisation technique was introduced. The MYLG results show an increment of 6.3% for HK1, 10.5% and 11.7% for HK2 and HK3 respectively, lower than discrepancy experienced in previous studies. The discrepancies reduce as the sequential scaling was reduced; hence, this optimisation method can be employed in further HOMER MYLG simulations to obtain more reliable capacity sizing. Additionally, HK2 and HK3 show similar techno-economic results with the cost of energy (COE) of $0.2/kWh, doubled the COE from the grid ($0.1/kWh). However, the life cycle cost of the proposed HESs are cheaper compared to the grid extension alternative. HK2 and HK3 design scenarios will achieve grid parity with 100% initial capital subsidy from the Government.

1. Introduction

1.1 Overview

Energy in the form of electricity, and water are both essential resources for every human on earth, and their efficient utilisation is crucial for a sustainable future. With the rapid economic and population growth, the provision of affordable electricity with less negative environmental impact is a major challenge. Similarly, the demand for clean water has risen, posing a shortage risk due to unavailability of power for water treatment in some remote regions. Hence, adequate provision and efficient management of electricity and water are vital in improving energy poverty and standard of living [1].

1.2 Problems and potential solution

About one-fifth of the world's population lacks access to electricity, with Asia and Africa were the most electricity-deficient [2]. In Africa, over 82% of the rural and 18% of urban dweller's lacks access to electricity, and a more significant percentage experiencing power outage due to insufficient generation capacity [2], [3]. In the case of water, small island faces the most significant challenges of quality water due to contamination from seawater, further worsen by the unavailability of affordable electricity for desalination [4]. Ameliorating this coherent menace between water and electricity has been deterred by the conventional mode of power generation and transmission. In most parts of the world, large power plant generates electricity far away from the demand and then transmits to the end-user through the power grids. Extending the existing grid to remote areas is often not cost-effective due to the considerable cost of construction, maintenance and power losses over long-distance [1]. Therefore, in generating power closer to load, the use of diesel-powered generators (Di-G) has been exploited in most off-grid regions [5]. However, there have been calls demanding the elimination of fossil fuel due to energy security and environmental concerns. Besides, the cost of importing diesel fuel to rural areas often increase its cost of energy (COE), creating an opportunity for Renewable Energies (REs) exploitation in remote areas [1], [3], [6].

However, REs are intermittent energy source that requires the support of reliable energy sources. Non-REs mostly from fossil-fuel sources and energy storage systems (ESSs) can help in filling the gap of the unreliability of REs, resulting in a combination of distributed energy resources (DERs) in power system called Microgrids (MGs) [5]. MGs refers to a small-scale group of DERs and loads operated in grid-connected or autonomous operation mode coupled with energy management systems and sophisticated control devices [7]. A random combination of different DERs in MG does not automatically lead to a lower cost of electricity rather careful selection and optimisation of DERs capacity while ensuring both load and supply matches at all time is required. In achieving this, Governments and private organisations have financed several real-life MGs [7][8][9][10] to investigate their feasibility in rural electrification.

1.3 Brief literature review

European Union (EU) funded the first MG project in Europe. The primary objective was to develop a comprehensive structure of a stable autonomous MG, serving as a model for entire Europe. These studies led to the successful installation of a novel MG on Kythnos Island in Greece [7], with many others inspired from it such as the NINES project in the United Kingdom (UK) [8], the first smart microgrid in the UK at Orkney Island [11], CESI microgrid in Italy [7] and ISET microgrid in Germany [7]. Studies in North America used a different mode of operation in MGs called "Consortium for Electric Reliability Technology Solutions (CERTS)" presented in Figure 1. In this mode of operation, a large thyristor (GG) switch was designed to seamlessly interface the small electricity grid with the utility grid using software programs allowing for a self-stabilising effect without the utilising high-end communication strategy employed by EU MGs [9]. However, CERTS will be economical unviable when the islanded region is far from the utility grid, motivating other kinds of research to ensure power quality delivery and fault control on isolated MGs without the use of thyristors. In this context, a novel solution in Japan was developed by coupling combined heat and power (CHP) system, solar photovoltaics (PV) cells, ESSs, wind turbines (WT) and biogas generators (BG) controlled with a traditional communication system (gateway means of communication). The project was implemented on Jeju's Island, which saw a substantial increase in wind penetration on the Island from 18 MW to over 200 MW [10].

However, small-scaled MGs have been studied in developing countries. An example is the laboratory scale MG at the Institution of Engineering and Technology (IIT), India [12]. The system uses a Pulse Width Modulation (PWM) inverter in power control and stability and Particle Swarm Optimization (PSO) algorithm-based fuel cells, requiring no complex communication systems

[12]. This technique has been employed in a MG installation in Africa at Ololailumtia, Kenya. It uses a 3 kW inverter in ensuring an active operating condition for a network consisting of a 2 kW WT, 2.42 kW solar PV and a 19.20 kWh battery (BT) storage [13].

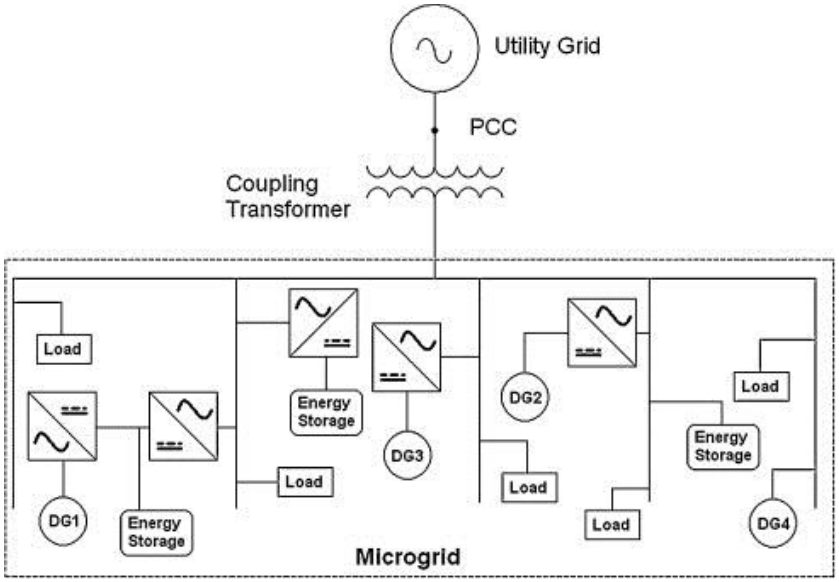

Figure 1: A typical microgrid schematic. DG1, DG2, DG3 & DG4 can be a variety of generators such as WT, Solar PV, Di-G and BG depending on the load's requirement (AC/DC) on the bus [7].

1.4 Research gaps and objectives

Significant accomplishments have been made in the implementation of MGs all over the world, supported mostly by Government funding, with little regards to the cost implications of construction which might be passed on to energy consumers as high COE. This led to the development of different software applications in simulating both large and small-scaled MG, to understand the technical and financial characteristics of MGs. Also, in estimating the influence of MGs on energy poverty and environmental issues. Several authors [14]–[20] as adopted Hybrid Optimisation Model for Multiple Energy Resources (HOMER) in this regard [21].

Outlying areas and villages without access to adequate electricity are predominant in developing countries. To investigate a possible solution in India, Rohit and Subhes (2014) varied different combinations of DERs to obtain a cost-effective solution for a village [14]. They used HOMER in getting the best-case scenario for the RE combinations and compared its financial implication to grid extension alternative. The blend of a small hydropower turbine (HT), PV, BG and battery (BT) created the best-case scenario with COE of $0.42/kWh compared to the extrapolated grid extension price of $0.44/kWh [14]. However, the provision of affordable electricity to a region will generally see continual growth in energy requirement over time due to a rapid increase in population and improved standard of living. Although studies from Rohit achieved a cost-effective system for the communities using a hybrid REs, which also resulted in less carbon emission. However, they did not estimate for the future increase in demand; this trend has been observed in most MGs optimisation [18]–[20]. Full details of all the studies is provided in Table 1.

A major constraint in using the load growth functionality (MYLG) in HOMER is capacity sizing. It is expected that the techno-economic result of both non-MYLG and MYLG be homogenous, but the homer optimiser is incompatible with the MYLG model requiring manual imputation of components capacity for MYLG simulations which usually lead to over scaling and high COE. An example of this the study by Kumar et al. (2018). They used a pre-defined scaling of (100-1000 kW) BG sizing in simulating 12 case scenarios in HOMER with the MYLG model. The result shows a COE of $0.17- 0.27/kWh [15]. Although Kumar et al. achieved a feasible system with relative low COE compared to some non-MYLG studies; they did not compare their designs scenario with

its non-MYLG model. Similarly, Aziz et al. (2019) used the MYLG model in investigating the optimum hybrid energy systems (HESs) for a village in Iraq, an increment of 17.9% for MYLG COE as compared to the non-MYLG simulation was obtained [16]. These two studies [15], [16] used a predefined scaling based on energy demand and could have achieved a different result if lower capacity scaling were used.

Hence, in addressing the constraints in rural electrification and the research gaps as described above, this study will investigate the techno-economic feasibility for the implementation of a cost-effective HESs to meet the growing demand for both electricity and water of remote areas by introducing a new technique for MYLG optimisation in HOMER. In addition, Sensitivity analysis to investigate the versatility of the HESs under different weather conditions using the village of Akassa in Nigeria as the study site.

Table 1.
Summary of both real-life and app-based MG projects selected for this study.

MG	Name/By	Location	Technology	Focus/Aim/Achievements	Refs
Real-life (mostly ongoing)	NTUA	Greece	PV,Di-G & BT	Developed CA,BS &PS	[7]
	CERTS	USA	GG & BT	Easy Integration of small DGs	[9]
	NINES, Shetland	UK	WT,Di-G,PV & BT	Novel ANM	[8]
	ORKNEY SG	UK	Several DGs & ESS	SG & ANM implementation	[11]
	CESI	Italy	ST,WT,CHP,PV & Di-G	Studying ACS	[7]
	ISET	Germany	Several DGs & ESS	Universalities & P-n-P concept	[7]
	Jeju, MG	Korea	WT, FC & Di-G	Increasing wind penetration	[10]
	Ololailumtia	Kenya	WT, PV & BT	Cheaper COE	[13]
	IIT, MG	India	PV, WT & FC	Inverter for power control	[12]
App-based	Mariya (2014)	Netherland	PV, WT & BT	RE for Water provision	[20]
	Rohit (2014)	India	HT,PV,BG,WT &BT	Cheaper COE using all RE	[14]
	Lau (2016)	Malaysia	PV, Di-G,FC &BT	Cheaper COE for PV/BT	[19]
	Aziz (2019)		PV, Di-G, BT & HT	More reliable MYLG results	[16]
	Kumar (2018)	India	PV, BG & DG	Multiyear load growth analysis	[15]
	Adefarati (2017)	South Africa	PV, WT, Di-G & BT	Lower NPC & COE	[18]

2. Location and energy demand

2.1 Location of study and motivation

The Akassa village, shown in Figure 2, was used for this study. Detailed properties of the village are presented in Table 2. An expanded map in Appendix 1 depicts the surrounding villages, Nun River, estuary and the Atlantic Ocean [22]. Akassa communities is an archipelago bounded by the Atlantic Ocean at the southern coast of Nigeria with brackish underground water (Figure 2). The river Nun and the Atlantic Ocean form an estuary at Akassa [23]. Ocean tides usually force brine up-river, contaminating its fresh surface water. Most people in the village drink the health-threatening brackish water because the imported freshwater from the city (180 km away) is expensive [24]. Currently, the village is off-grid, and only a few households, medical centre, and schools use small-scale generators ranging from 1-3 kW. The nearest connection to the national grid from the village is 240 km away posing the major constraint of connecting the village to the utility grid [24]. Therefore, water desalination and provision of affordable electricity will increase the socio-economics and quality of life in this region.

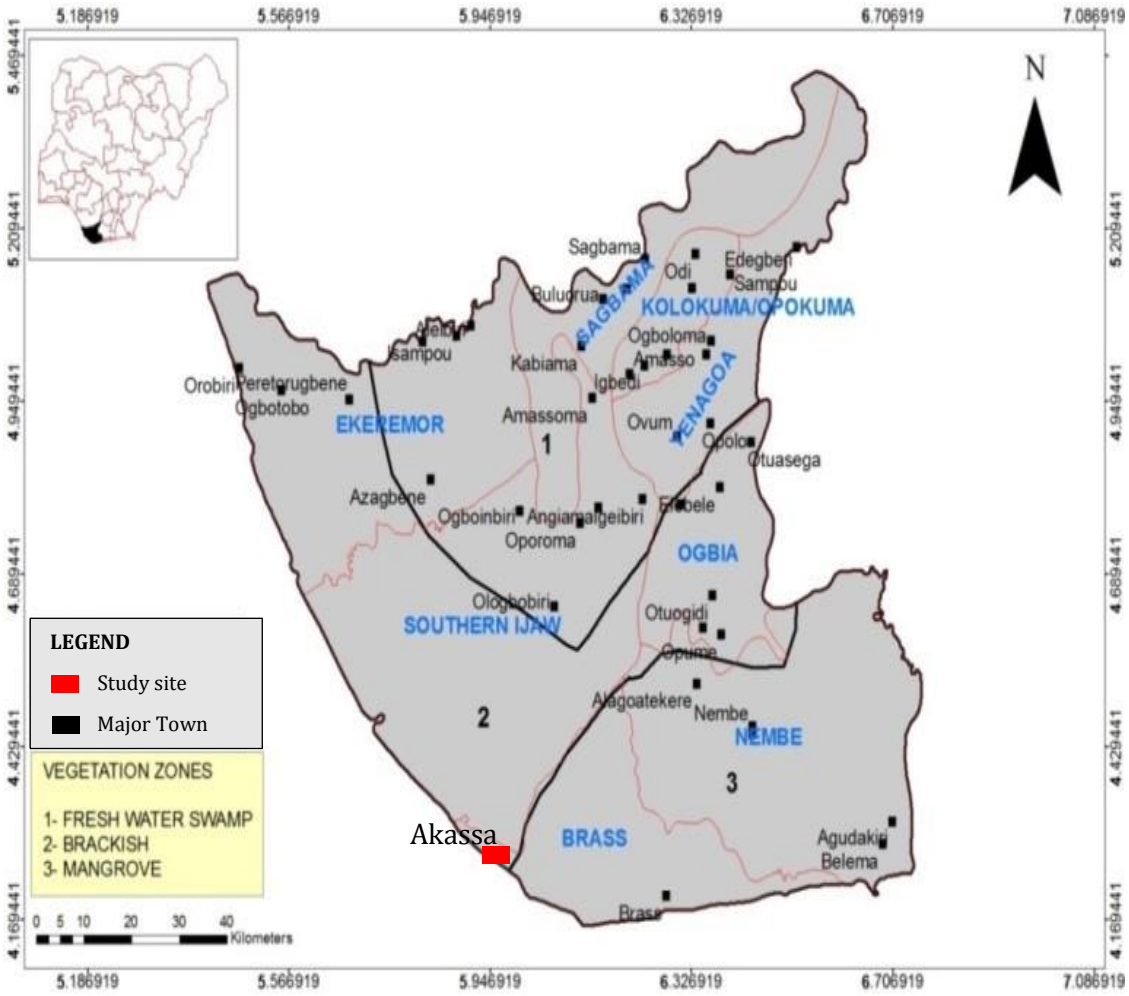

Figure 2: Map of the research location. The map shows the vegetation zones for Bayelsa state in Nigeria with the research location falling into the brackish zone [22].

Table 2.
Detailed properties of Akassa village [22]–[24].

Property	Description
Village	Akassa
Region	Bayelsa
Elevation	4.55 m
Country	Nigeria
Season	Wet and Dry
Longitude	6°04'08.4"E
Latitude	4°19'22.8"N
Population	4500
Major Occupation	Fishing
No of Households	987
Schools	2
Medical Centre	1
Underground Water	Brackish
Distance from grid	240 km

2.2 Load assessment.

The load estimation of remote areas is often challenging due to unavailability of electricity consumption data. Therefore, load modelling was used to estimate the electricity demand in this study. The load modelling was done by categorising the load types into two categories: primary and deferrable load:

2.2.1 Primary load

Primary loads are the electrical loads that must be met at a particular time to avoid failure of the grid [14]; they include the community and industrial loads shown in Table 3. The community's load was estimated by counting the number of appliances for a small sample of houses and then aggregating for all population/households in the village. The consumption pattern was estimated using the load pattern for a typical village in Nigeria with consideration for both dry and wet seasons [25]. Similarly, modelling of industrial load pattern was done but with a different load pattern based on the working hour of typical village industry. Figure 3 and Figure 4 show the estimated overall power demand and seasonal variation.

Table 3.
The appliances estimation for both the primary and deferrable load.

	Load type	Examples	Average Power (W)	Quantity	Total Power (KW)	Usage hours/day		Energy (KWh)	
						Wet	Dry	Wet	Dry
						Apr - Oct	Nov -Mar	Apr - Oct	Nov -Mar
Primary	Community (incd. School, Medical center)	Lighting(Led + CFL)	25	500	12.5	8	7	100	87.5
		Air conditioning(Fans)	120	60	7.2	3	8	21.6	57.6
		TV	133	120	15.96	7	7	111.72	111.72
		DVD	25	85	2.125	5	6	10.625	12.75
		Phones	10	400	4	5	5	20	20
		Radio	40	162	6.48	10	10	64.8	64.8
		refrigeration	800	10	8	24	24	192	192
		Computer	150	24	3.6	9	9	32.4	32.4
		Miscellanous	10	4500	45	1	1	45	45
		Total			**104.865**			**598.15**	**623.77**
	Industrial	Lighting(Led + CFL)	25	8	0.2	12	12	2.4	2.4
		Sawmills	9000	2	18	9	9	162	162
		Grinding Machine	5000	2	10	12	12	120	120
		TV	130	1	0.13	10	10	1.3	1.3
		Radio	40	4	0.16	10	10	1.6	1.6
		Fan	120	3	0.36	5	10	1.8	3.6
		Others	500	10	5	9	9	45	45
		Total			**33.85**			**334.1**	**335.9**
Deferrable	Agricultural	Irrigation System	1800	9	16.2	0	3	0	48.6
	Desilanation	RO-Plant	5000	1	5	4	4	20	20
		Total			**21.2**			**20**	**68.6**

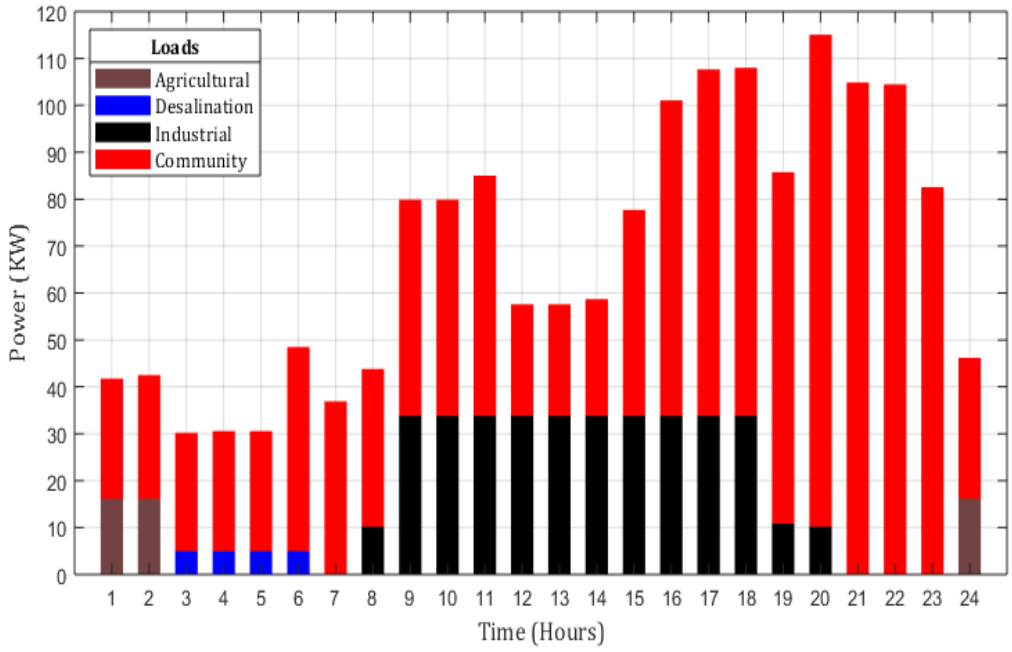

Figure 3: Hourly power demand for a typical day in the dry season. Peak power of 118 kW in the evening (20:00) when everyone turned-on their devices at the same time, which is rare in reality. Therefore, the diversity factor was applied.

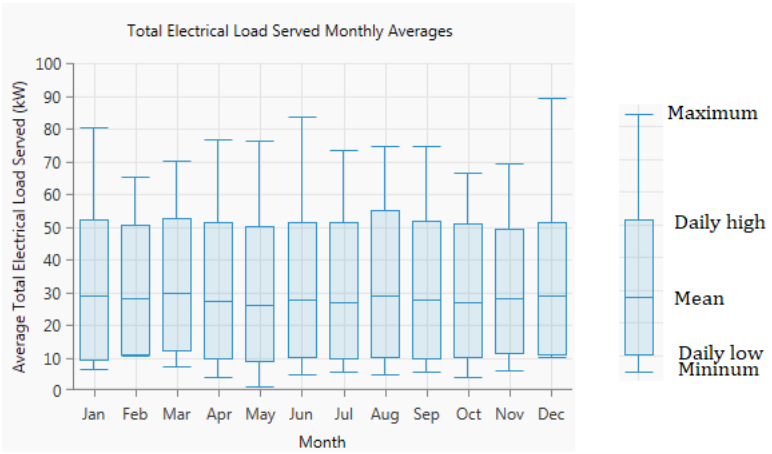

Figure 4: The seasonal load demand for the first year. The peak average load demand experience in December (84 kW), a reduction to the estimated due to the application of diversity factor. The hottest months (Dec-Jan) experienced higher energy consumption due to an increase in the usage of cooling appliances.

2.2.2 Deferrable load

These are electrical loads that must be met within a specific period, although the exact time is not important [14]. Both the agricultural and desalination loads (Table 3.) were taken to be deferrable. The pumping of water for irrigation can wait for a while, as well as the desalination of water provided storage tanks are installed. The pattern of a deferrable load is dependent on the availability of energy which may vary from time to time; therefore, the energy consumption can be at any time of the day usually at a period when all the primary loads have been met.

2.2.3 Water requirement

The estimated average water demand per capita consumption for a rural community in Nigeria was 2.1 – 2.6 l/day [26]. Hence, Akassa village drinking water demand will be in the ranges of 9500-12000 l/day. A medium-sized reverse-osmosis system for brackish water with a feed rate (4375 l/h, 80% recovery) and a production capacity of 3500 l/h may consume 20 kWh/day for the production of 14000 l/day with an average power demand of 4 kW [27]. This power demand was used to estimate the power requirement for water desalination, as shown in Table 3.

2.2.4 Load growth (MYLG) and diversity factor.

Annual population growth of 3% was experienced in Nigeria over the last two decades [28], [29]. This is taken to be the yearly load growth (MYLG = 3%) because the population growth influences the load growth and water consumption. Also, a situation whereby all appliances were used at the same time rarely happens. Realistically, the magnitude and usage time varies periodically. Therefore, the application of a random variability to account for the diversity factor can make the load pattern more realistic. 20% day-to-day and 15% time-step-to-time-step variability was applied. The effect of both MYLG and diversity factor after 25 years is shown in Figure 5.

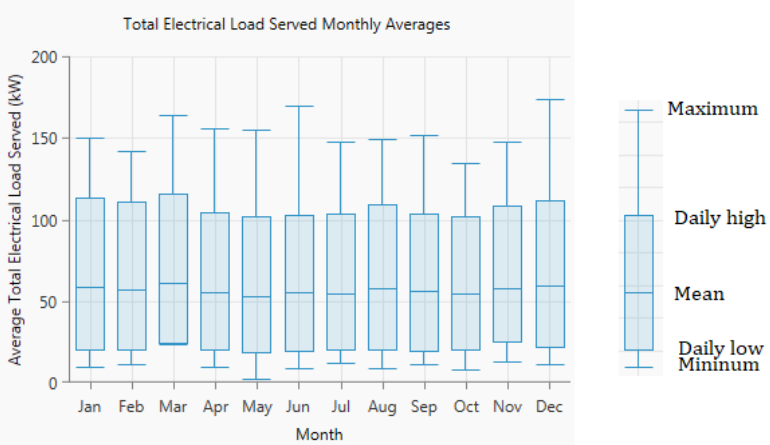

Figure 5: Load seasonal variation after 25 years. This shows the average peak power doubled compared to the first-year primary load (84 kW to 175 kW in December) in Figure 4.

3. Methodology

3.1 Research philosophy and data correction

The framework for the research methodology is shown in Figure 6, which was specifically developed for this project. The project started with an initial on-site assessment comprising of the load estimation as described in the previous section, followed by resource assessment. The metrological data (solar radiation, wind speed and precipitation) for Akassa (4°19'22.8"N 6°04'08.4"E) was obtained from the archive of National Aeronautics and Space Administration (NASA) in hourly timescale [30]. In this data, completeness and consistency of observation over a very long time is the major issue. MATLAB software was used in removing the fields without value. In addition, individual correction factors were applied to the resources power output. The location is a rural area without tall buildings and mountains; therefore, a corrections factor (deduction) of 3% was applied to PVs power output, accounting for shading from trees. Wind resource was not used in the simulation, so no correction factor needed. The hydrokinetic resource was modelled using the precipitation data to give the complete monthly average water speed for a year. Sensitivity parameters for the resources were estimated to account for

uncertainty in the weather. The data were fed into HOMER where the modelling, optimisation and simulation were done. The most suitable (optimal) system configurations were selected based on its life-cycle cost and COE. The post-homer analysis was conducted to determine the accomplishments of the proposed HESs by comparing it with grid extension alternatives, results from previous studies, limitation and possible solutions.

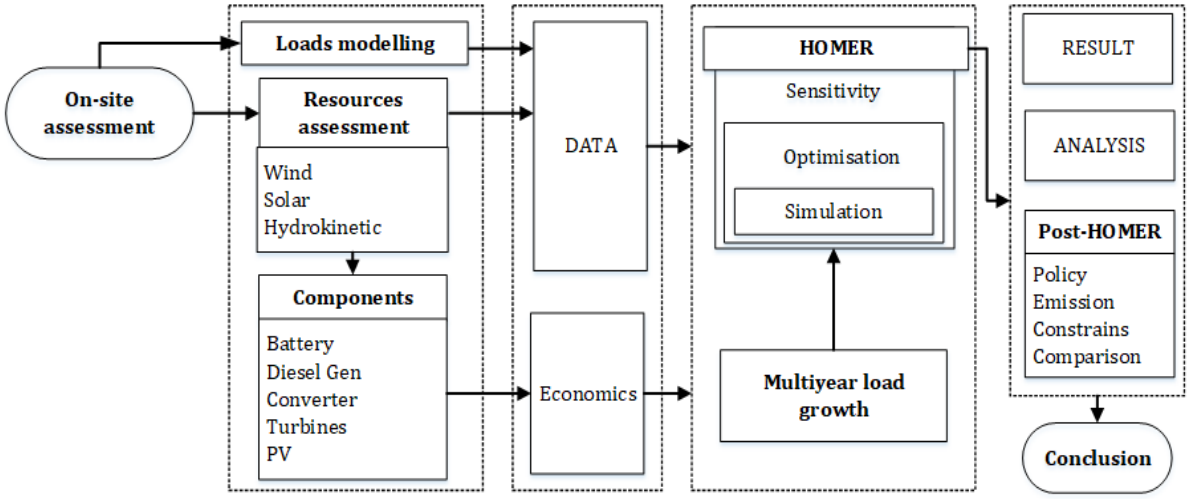

Figure 6: flowchart for the research methodology. This was developed to show the processes taken for this project.

3.2 Resource assessment

3.2.1 Solar

The monthly average solar radiation (MASR) dataset collected from NASA [30] is presented in Figure 7 The MASR ranges from 3.1-5.24 kWh/m²/day with the lowest radiation experienced during the raining months (May to September). A gradually rise during the dry months (October to April) reaching the peak in January. The daily clearness index denoting the ratio of global irradiance at the surface falling on a horizontal plane (GHI) to the extra-terrestrial global irradiance in the horizontal plane [31] was also observed to be in proportion with the daily radiation showing a relatively good solar resources in the location.

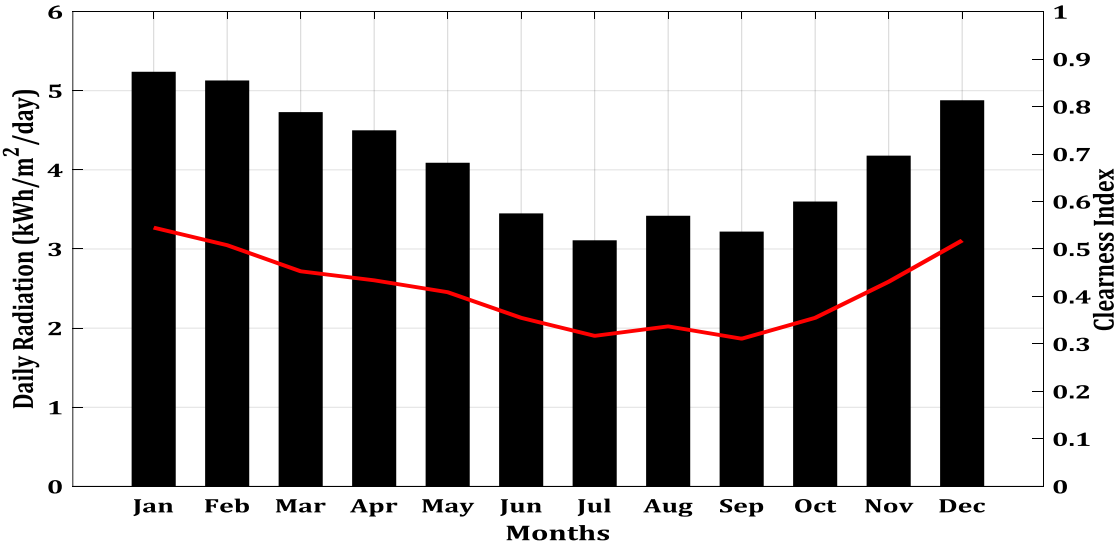

Figure 7: Monthly average solar GHI for 22 years with the red line denoting the clear index. High radiation during the dry seasons (October - April) and drops in radiation during the rainy (May - September) (Data source: NASA [30]).

3.2.2 Wind

The wind dataset obtained from NASA [30] at an elevation of 50 m is presented in Figure 8 as a Weibull probability distribution (WPD). The WPD can be used to fit a vast collection of recorded data in evaluating local wind speed probability [32]. It is based on two parameters scale (k), and shape (λ). The scale factor denotes how windy the location is, while the shape parameter denotes how peaked the wind is (usually between 1 - 3). Small λ indicates very variable winds, while large λ characterised constant winds [32]. MATLAB was used to fit WPD with resulting parameters shown in The annual average wind speed obtained (3.07 m/s) was considerably low for the minimum required wind speed (cut-in speed)of most WT, with very low probability of obtaining higher wind speed as observed by the values of the k (2.489 m/s) and λ (2.145) , Hence the wind resource was neglected in the HESs simulation.

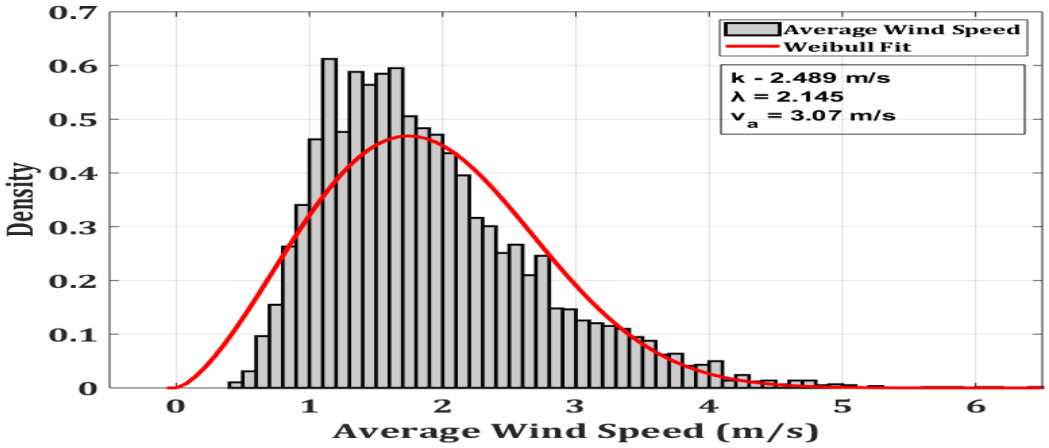

Figure 8: Weibull probability distribution for the wind speed of 22 years (1991 - 2013). The red line is the Weibull fit and resulting parameters on the graph (shape (λ), scale (k) and mean (v_a)). (Data source: NASA [30]).

3.2.3 Hydrokinetic (HK)

[23], [24] has identified the Nun river/estuary as a potential site for implementation of hydrokinetic resources with an estimated potential of 6 MW. Hydrokinetic turbines (HKTs) are similar to the conventional hydropower turbines (HTs) but with the neglection of the available head. The measured annual average of the water speed was 1.5 m/s at a depth of 20 m [23]. Monthly water flow rate data was not available for this location; hence, this study used precipitation, temperature and humidity data obtained from NASA to model the monthly average water speed based on the annual average of 1.5 m/s in correlation with the wet and dry season as shown in Figure 9 [21], [23], [24], [30].

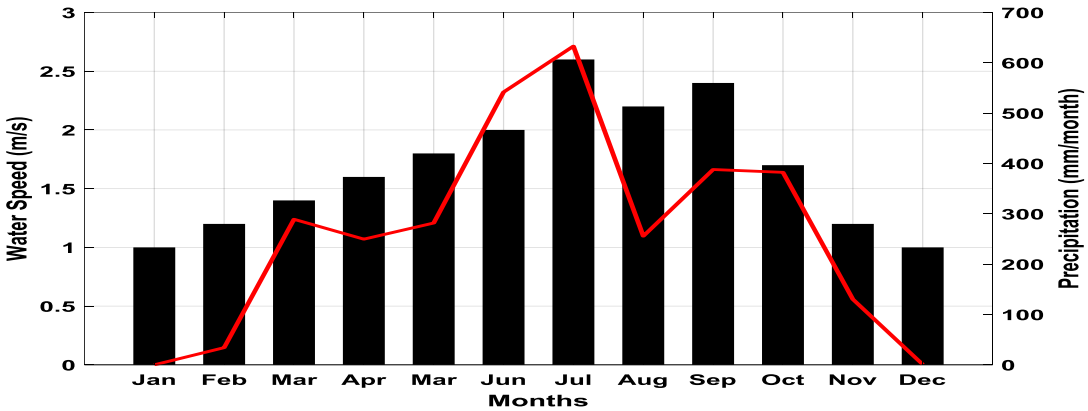

Figure 9: Monthly average water speed and precipitation. Model using data obtained from NASA and the measured average water speed of 1.5 m/s. High water speed during the wet seasons and drop during the dry seasons (Data source: NASA [30]).

3.3 Components assessment

Table 4. presents the optimised components costing based on International Renewable Energy agency (IRENA) recommendations and manufacturer's pricing, to give a good approximation of the location scenario.

Table 4.
The total economics of the components used in the simulation.

Component	Capital Cost	O/M cost (Annual)	Lifetime	Refs
PV	$2000/kW	$10/kW	20 years	[21],[33]
HKT	$350/kW	$5/kW	10 years	[21],[34]
BT	$300/kW	$10/kW	10 years	[21],[36]
Di-G	$500/kW	$10/kW	15000 hours	[21],[37]
Bi-Con	$3/kw	$2/kW	15 years	[21],[33]

NB: Capital cost = Replacement cost

3.3.1 Solar Photovoltaic cell (PV)

PV converts the solar resource into electricity. The initial capital cost was estimated to be $2000/kW, which includes the cost of the shipment and full installation with no tracking system. A PV system without tracking system will require little annual operational and maintenance (O/M) cost, taken to be $10/kW/year [21], [33]. The power of PVs was calculated in HOMER using equation (1) [21].

$$P_{pv}(t) = Y_{pv} D_{pv} \left[\frac{i_T(t)}{i_s}\right] \left[1 + \alpha_p (T_c - T_s)\right] \quad (1)$$

Where Y_{pv} - PV module rated power output (kW); D_{pv} - derating factor (%); $i_T(t)$ - global solar radiation incident on the PV module kW/m^2); α_p - temperature coefficient of the PV (%/°C); T_c - cell temperature of the PV module; T_s - cell temperature of the PV module at the standard condition (25°C).

3.3.2 Hydrokinetic turbine (HKT)

HKT harnesses the kinetic energy (KE) of moving water without the need for dam or penstock. The energy extraction of HKT is analogous to that of a WT. However, water is approximately 800 times denser than air; therefore, an HKT will generate more electricity than a WT of the same diameter. Additionally, Hydrokinetic resources have less environmental impact and variability compared to a wind resource. A 40 kW Darrieus hydrokinetic turbine (DHKT) was used in this study due to its suitability for low-velocity application [21]. Capital and O/M costs are presented in Table 4. The DHKT's power curve (Figure 10) shows how much power was generated at different water speeds. The turbine's power (P_{HT}) at each time step (hours) and the annual electricity generated ($E_{HT,annual}$) was calculated in HOMER using equation (2) and (3) [21], [35].

$$P_{HT}(t) = 0.5 * \rho_{water} * A * v^3 * C_p * \eta_{HT} \quad (2)$$

$$E_{HT,annual} = \sum_{t=1}^{8760} P_{HT}(t) * t \quad (3)$$

Where ρ_{water} - density of water (≈ 1000 kgm^{-3}); A - area of the turbine (m^2); v^3 - water's speed (m/s); C_p - performance coefficient; η_{HT} - efficiency of the overall hydrokinetic system (%); t – time (hours).

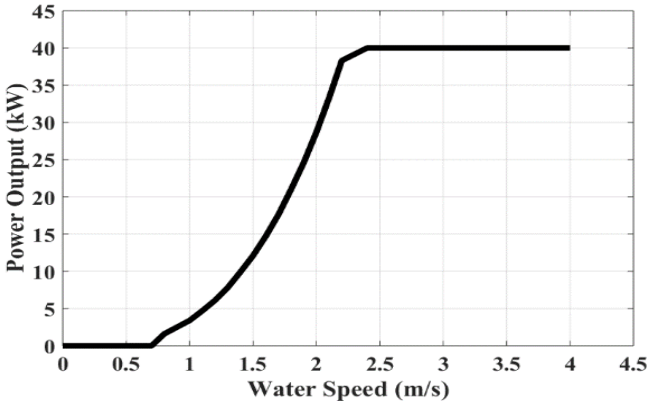

Figure 10: HKT's power curve. This shows the power obtainable at each water speed for the HKT (Data source: [21]).

3.3.3 Battery (BT)

In this study, the tubular flooded lead-acid BT was considered due to its availability and cost. The battery's behaviour is dependent on the dispatch strategy used in the simulation; however, a customised version state of charge (SOC) model for the proposed study was used in determining the technical variables of the battery during the charging-discharging state as shown in Appendix 2[21], [27]. Costing and technical parameters were taken from the manufacturer's datasheet [21], [36] and optimised based on IRENA's recommendation for the located (Table 4.).

3.3.4 Diesel generators (Di-Gs)

The Di-Gs serve as a backup energy source in case all the resources and the battery outputs cannot meet the required load demand. Based on the required peak load of over 100 kW, two Di-Gs (Gen50 - 50 kVA and Gen100 - 100 kVA) were selected. The initial cost was obtained from the manufacturer [21], but the O/M costs are significantly dependent on the price of the fuel (diesel) shown in Table 4. The diesel price is taken to be \$1/litre, which includes the cost of transportation to the village [37]. The total annual fuel consumption of the system $F_{Di-G,annual}$ $(litres/year)$ is modelled using equations (4) and (5) [15], [21].

$$F_{Di-G}(t) = \lambda_1 P_{Di-G_{out}} + \lambda_2 P_{Di-G_{rated}} \quad (4)$$

$$F_{Di-G,annual} = \sum_{t=1}^{8670} F_{Di-G}(t) \quad (5)$$

$\lambda_1 -$ Generator fuel slope (L/hr/kW); $P_{Di-G_{out}} -$ Di-G output power (kW); $\lambda_2 -$ Generator fuel intercept coefficient (l/hr/kW); $P_{Di-G_{rated}} -$ rated capacity of the generator (kW).

3.3.5 Converters and operating algorithm (Bi-Cons)

Bi-Cons are the devices that convert DC to AC and vice versa. These devices are usually embedded with the operating algorithms called dispatch algorithms (DAs). The DAs make the decisions of which different component combinations to operate in meeting the required load at each time step. This study employed two DAs during simulation: load following (LF) and cycle charging (CC). In CC mode, Di-Gs operates at the rated or full capacity equal to battery power charge limit to meet the primary load, supply excess energy to the deferrable load and ESSs. The Di-Gs will not stop until the ESSs are fully charged. Under LF, Di-Gs operate at a capacity required to serve the primary loads only while ensuring operational reserve requirements are met, deferrable loads and ESSs demand are left until REs are available and sufficient enough [15], [21]. The two DAs specifically for the modelled HESs are presented in Figure 11.

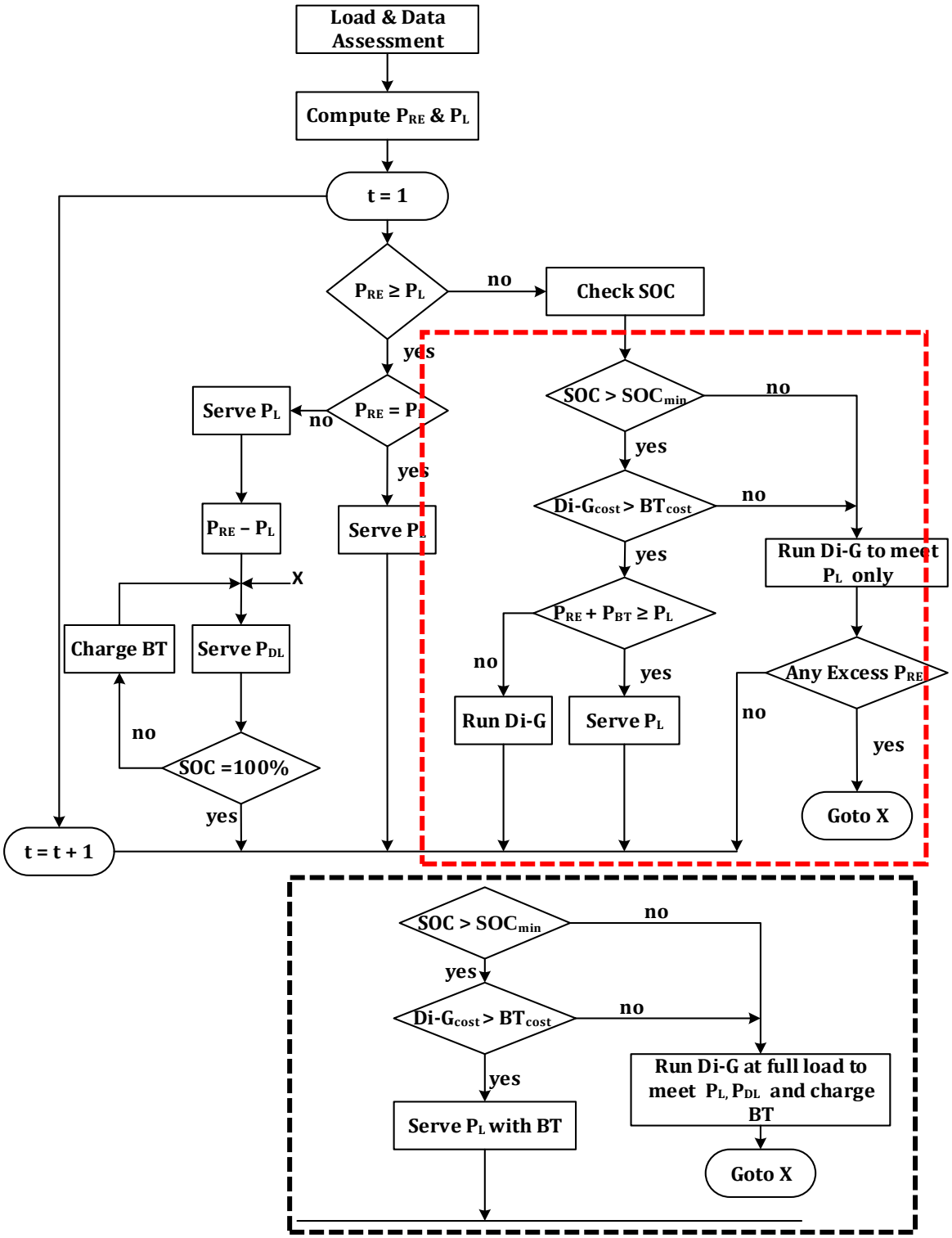

Where t – time step (hourly); P_{RE} – Total RE hourly power; $P_{RE} = P_{HKT} + P_{PV}$; P_{PV} – PV hourly power output; P_{PV} - PV hourly power output; P_{HKT} – HKT hourly power output; P_T – BT hourly power output; P_L - Primary load power; P_{DL} - deferrable load power; $Di\text{-}G_{cost}$ - cost of running HKT; BT_{cost} – cost of running BT; NB – All parameters are hourly time step.

Figure 11: The DAs flow chart. The upper flowchart section represents the DA for the LF strategy, and the CC strategy can be obtained by replacing the red dotted section in LF flowchart with the black dotted section.

3.4 The hybrid system

The resources and components assessment explained above were used in designing three HES scenarios in HOMER as shown in Figure 12. The three scenarios are (HK – one HKT; HK2- two HKT and HK3 – three HKT) simulated for 25 years. The possibility for grid extension was added to the design, and the characteristics of the grid extension are presented in Appendix 3.

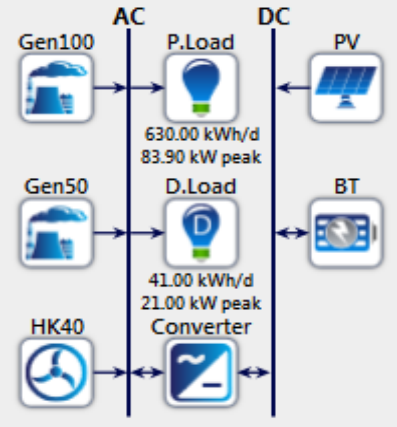

Figure 12: The complete hybrid system modelled in HOMER software. This shows all the components and configuration coupled with the grid extension.

3.5 Economics assessment criteria

REs often require a significant amount of initial capital and low O/M cost while non-REs incur small initial capitals and high O/M over its lifetime. Due to this discrepancy between these two DERs, the life-cycle cost assessment is an appropriate metric in comparing HES configurations. HOMER uses the total Net Present Cost (NPC) in representing the lifecycle cost of the system. NPC combines all the cost and revenue accrued during the project lifetime with the future cash flow discounted back to the present value using an annual interest rate [14], [21]. However, the cost of energy (COE) has been the convenient metrics used in studies [14], [15], [18], [19], but HOMER gave more preference to total NPC during ranking because COE is somehow disputable. COE divides the annualised cost of the system by the total electrical load served (useful energy) rather than the electrical load demand or total electricity generated [21], causing an inconsistency in scenarios with excess generation and unmet electrical loads. The total NPC and COE were calculated in HOMER using equations (6), (7) and (8) [15], [21]:

$$C_{NPC} = \frac{C_{ann,total}}{CRF(i, N_{Proj})} \tag{6}$$

Where $C_{ann,total}$ – total annualized cost ($/year), CRF - capital recovery factor, given by Eq. (6).

$$CRF(i, N_{Proj}) = \frac{i(1+i)^{N_{proj}}}{(1+i)^{N_{proj}}} \tag{7}$$

Where i - annual real interest rate (%), and Nproj - lifetime of the project (years).

$$COE = \frac{C_{ann,total}}{E_{primary} + E_{deferrable}} \tag{8}$$

$E_{primary}$ and $E_{deferrable}$ are the total amounts of primary and deferrable load, respectively, that the system served per year.

4. Results

4.1 Pre-optimisation technique and results (Non-MYLG)

Due to the incompatibility of the MYLG model with HOMER's optimiser, a pre-optimisation strategy was developed to avoid oversizing. This involves a pre-optimisation using a single year simulation (non-MYLG). The resulting capacities from the non-MYLG simulation was used in scaling the capacity requirement for the MYLG model. This was done by applying a sequential scaling size (up and down) to the optimisation capacity results obtained from non-MYLG simulation as shown in Table 5.

Table 5.
Non-MYLG optimisation results. The optimised components capacity in this result were used in scaling the range of components capacity during the MYLG simulations. The optimisation capacities were rounded and a sequential scaling (± ten steps up and down) was applied to MYLG components sizing.

							MYLG scaling (steps up and down)		
	PV (kW)	Gen50 (kVA)	Gen100 (kVA)	BT (kWh)	Bi-Con (kW)	COE ($/kWh)	PV (kW)	BT (kWh)	Bi-Con (kWh)
HK1	88.8	0	100	389	40.3	0.316	80 (±5)	400 (±50)	40 (±1)
HK2	35	50	100	90	25	0.18	30 (±10)	100 (±10)	30 (±5)
HK3	42	50	100	112	31.4	0.17	40 (±10)	100 (±20)	35 (±5)

NB - During multiyear the Di-Gs (Gen50 and Gen100) were run in all simulations

4.2 MYLG optimisation results

Table 6 and Table 7 show the techno-economic optimisation results from HOMER respectively. For scenario HK1, the most suitable configuration obtained for the location was PV-Gen50-Gen100-BT-HK hybrid system. This hybrid system is composed of one HKT (40 kW), 95 kW of PVs, both 50 kVA and 100 kVA Di-G supplemented with a 300 kWh batteries bank operated using LF DA. During the first year, 306,175 kWh/year (In excess - 15.2%) was produced. The two REs produced 84.4% (PVs - 43.2% & HKT - 41.2%) while the Gen50 produced 15.4% with an insignificant 0.2% production from Gen100 during this year as presented in Figure 13. Due to gradual increase in total electricity production to meet the growing load demand, the production during the last year (25th year) increased to 501,927 kWh (In excess – 1.26%) of which the RE s contributed 51.5% (PV – 26.4% & HKT 25.1%) while the non-REs produced a combined of 48.5% (Gen50 – 24.6% & Gen100 – 23.9%). The economic results for this system show a total NPC of $1.77 million and a COE valued at $0.336/kWh (Table 7.).

For the HK2 design scenario, the optimal combination composed of 40 kW PVs, both Gen50 and Gen100, supplemented by 100 kWh batteries bank operated using LF DA. In this case, the HKT generates 70% of the total electricity production during the first year, Gen50 and PVs produced 13% and 15% respectively while Gen100 contributed 0.48% of the total output as presented in Figure 13. The electricity production was 358,628 kWh/year (In excess – 30%) for the first year (Table 6.). To meet load growth, the total energy production increased gradually and attained 538,874 kWh/year at the 25th year with excess of 6.8% for which the two REs (HKTs and PVs) contributed 46.8% and 10.3% respectively while the non-REs (Gen50 and Gen100) produced 19.4% and 23.5% respectively. The economic results in Table 7. show a total NPC of $1.07 million and a COE equal to $0.201/kWh.

Like the first two scenarios, the most suitable configuration for HK3 design scenario is the PV-Gen50-Gen100-BT-HK hybrid system. It required the combination of 50 kW PVs, both Gen50 and Gen100 and battery bank of 120 kWh operated by the LF DA. 477,925 kWh/year (In excess – 48%) electricity was produced during the first year and 611,117 (In excess – 12.7%) in the last year (Table 6.). During this time, PV production reduced from 14.6% to 11.4%, HKTs production

also decreased from 79.2% to 61.9%. The two non-RE Sources experienced an increase in output over the years with Gen50 increasing from 6.17% to 13% and Gen100, from 0.1% to 13.7% (Figure 13). The economic results for this combination show a total NPC of $1.07 million and a COE valued at $0.199/kWh (Table 7.).

Table 6.
MYLG technical optimisation result. The technical details for the most suitable hybrid systems with the DAs.

								TEP (kWh) (EP (%))	
Cases	**PV (kW)**	**Gen50 (KVA)**	**Gen100 (KVA)**	**BT (kWh)**	**Bi-con (kW)**	**DA**	**RE Frac (%)**	**1st year**	**25th year**
HK1	95	50	100	300	42	LF	64.89	306,175 (15.2)	501,927 (1.26)
HK2	40	100	50	100	30	LF	66.9	358,628 (30)	538,874 (6.8)
HK3	50	50	100	120	35	LF	78.38	477,925 (48)	611,117 (17.7)

TEP - (Total Eletricity production); EP - (Excess Production)

Table 7.
MYLG economics optimisation result.

Cases	NPC ($)	COE ($/kWh)	O/M ($/yr)	I. capital ($)
HK1	1,769,225	0.336	82,033	466,600
HK2	1,068,171	0.201	51,398	252,000
HK3	1,067,048	0.199	48,084	303,500

I.capital - Initial Capital

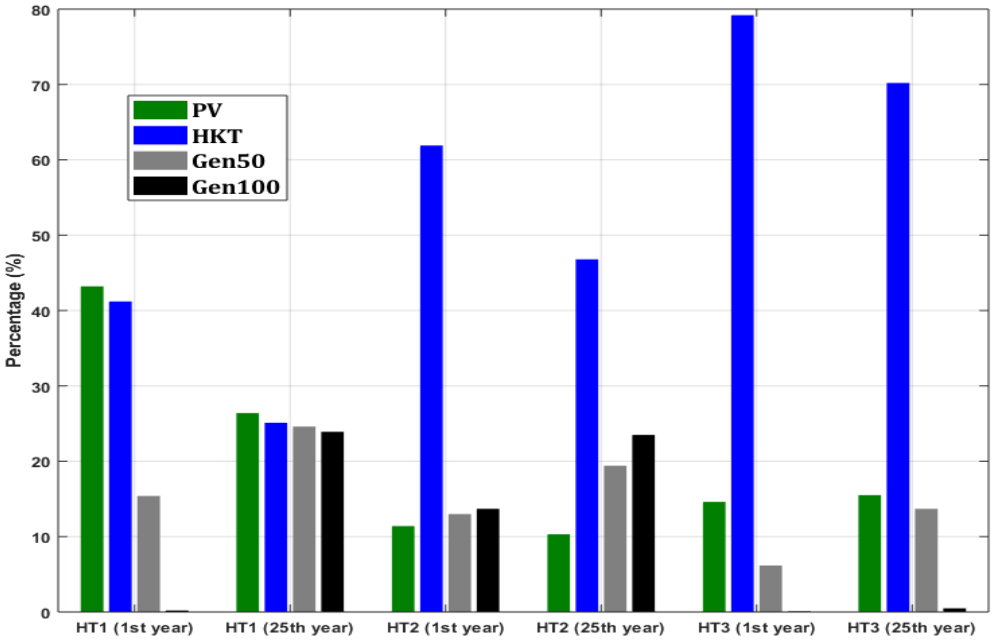

Figure 13: The percentage generation of each generating set in the first and last year of the project for the three scenarios. In the first year, HK produced a significant amount of energy during the first year for all the scenarios while Gen100 produced an insignificant amount. Due to load growth, Gen100 increase production gradually over the years.

4.3 Sensitivity analysis

4.3.1 Sensitivity parameters

Intermittency is inevitable for MG with REs penetration. These variabilities were taken into account to investigate the effect of change in resource parameters on the three design scenarios. The scaled parameters chosen are presented in Table 8.

Table 8.
Sensitivity analysis parameters.

Resource	Sensitivity Parameter	Scaled Values
Solar (kWh/m2/day)	AA Daily radiation	3,3.5,4.13*,4.5 & 5
HK (m/s)	AA Water speed	1,1.5*,2 & 2.5 (m/s)

* - Expected Value; AA - Annual Average

4.3.2 Sensitivity results

Figure 14 shows the sensitivity analysis result for the HK1. In this case, only one system configuration (Gen50-Gen100-PV-HK-BT – all black grid) is possible, irrespective of the solar radiation and water speed. A gradual decrease in both the total NPC and COE as the value of the scaled resources increase, both reaching a minimum at the maximum values of the scaled solar radiation and water speed. The results of the sensitivity for both HK2 and HK3 are presented in Figure 15 and Figure 16, respectively. For these scenarios, two optimal system configurations are possible (red and black grid), depending on the available resources. The red grid on the graphs represents the combination of Gen50-Gen100-PV-HK-BT while the black grid represents the Gen50-Gen100-HK-BT. The result obtained for the second scenario (HK2) proposed the combination of Gen50-Gen100-PV-HK-BT when the water speed is less than 1.55 m/s and Gen50-Gen100-HK-BT otherwise. The least NPC and COE were both attained for Gen50-Gen100-HK-PV-BT at the value of the maximum resources. The Gen50-Gen100-HK-BT combination is independent of the solar radiation due to the elimination of the PVs but still obtained the least NPC and COE at the maximum water speed (Figure 15). Figure 16 shows the sensitivity result for HK3, which has a similar pattern to HK2, but the Gen50-Gen100-HK-PV-BT design was proposed at a water speed less than 1.8 m/s. In addition, HK3 experienced lower NPC and COE compared to HK2, even at the same scaled resource parameters.

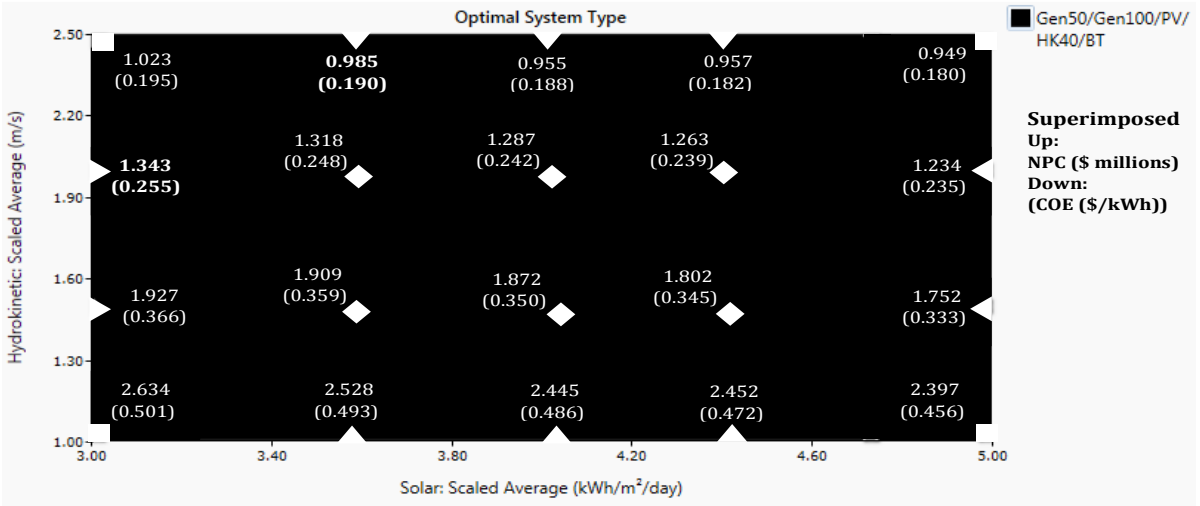

Figure 14: Sensitivity result for HK1 over a range of solar radiation (3 – 5 kWh/m²/day) and water speed (1- 2.5 m/s). The entire graph is black denoting only the combination of Gen50-Gen100-PV-BT-HK. The total NPC and COE reduce as both solar radiation and water speed increases.

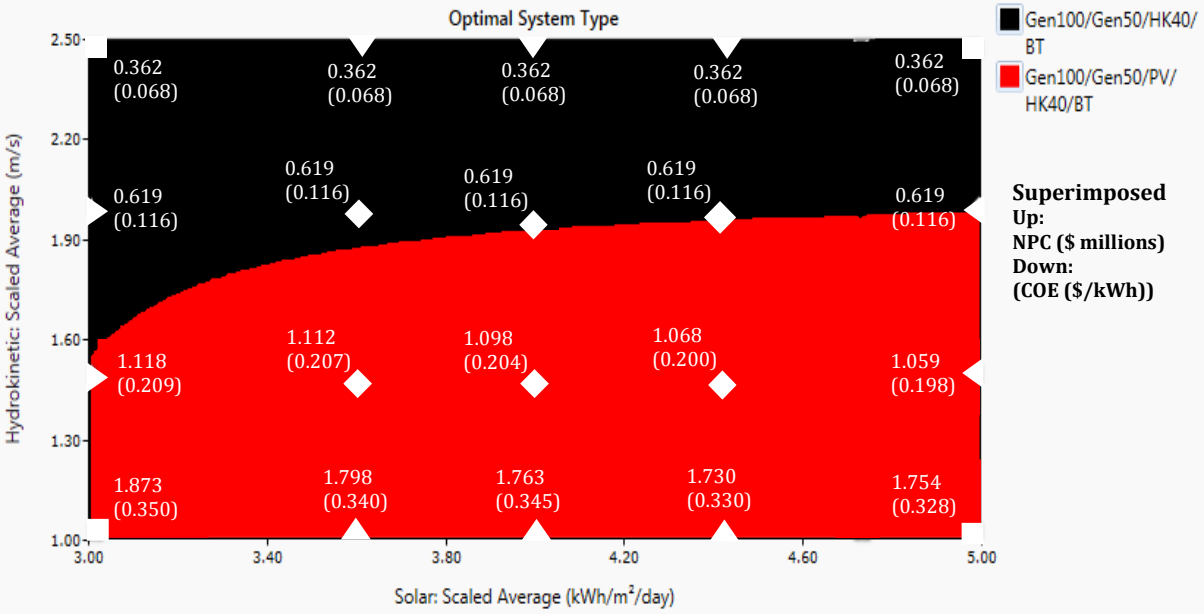

Figure 15: Sensitivity result for HK2 over a range of solar radiation (3 – 5 kWh/m2/day) and water speed (1- 2.5 m/s). The graph shows the possibility of two configurations (red and black). For the Gen50-Gen100-PV-HK-BT (red) configuration, the total NPC and COE decrease as both solar radiation and water speed increase while Gen50-Gen100-HK2-BT (black) economic value is independent of solar radiation.

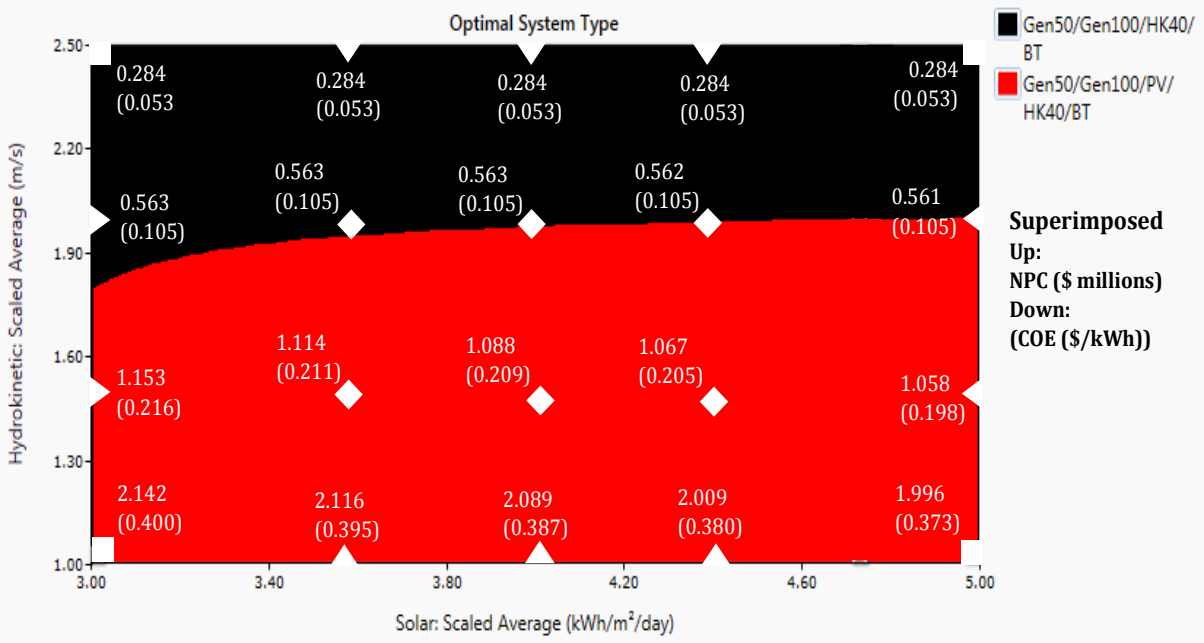

Figure 16: Sensitivity for HK3 over a range of solar radiation (3 – 5 kWh/m2/day) and water speed (1- 2.5 m/s). The graph shows the possibility of two configurations (red and black). For the Gen50-Gen100-PV-HK-BT (red) configuration, the total NPC and COE decrease as both solar radiation and water speed increase while Gen50-Gen100-HK-BT (black) economic value is independent of solar radiation.

5. Discussion

5.1 Grid extension (GE)

GE is an alternative widely considered by the Governments in the electrification of communities is the connection to the grid. The LCOE for grid electricity across Nigeria is currently $0.1/kWh [37] which is cheaper than the COE ($0.199 - $0.336/kWh) from the HESs. The arrival of grid electricity in rural communities is a potential threat to the implementation of the HESs. Therefore, the life cycle cost comparison of the HES with grid alternative is essential in determining the most economical in the long run.

The breakeven distance (BGED) is achieved when the total NPC of a HES is equal to that of the NPC of GE [21]. The BGED was estimated for the three case scenarios, and the result is presented in Figure 17. BGED is the point of interception between HES's total NPC and the GE lines. The figure shows that BGED for the HK1 scenario is 92.8 km, while HK2 and HK3 are 37.4 km and 36.7 km respectively. As previously discussed, the nearest grid connection point from Akassa is 240 km [24]; hence, it can be deduced that the total NPC for the GE is more expensive than that of the HESs proposed in this study (240 > 92.8, 37.4 and 36.7). Therefore, the three HESs are more economically feasible than GE in the long run. In addition, the grid electricity in the developing country is usually unreliable with frequent capacity shortage, power cuts and energy loss over long transmission distance [38]. The simulated scenario is simulated to be reliable with 0% unmet load and capacity shortage for the entire 25 years of the project. Therefore, any of the three scenarios are more technical efficient compared to GE.

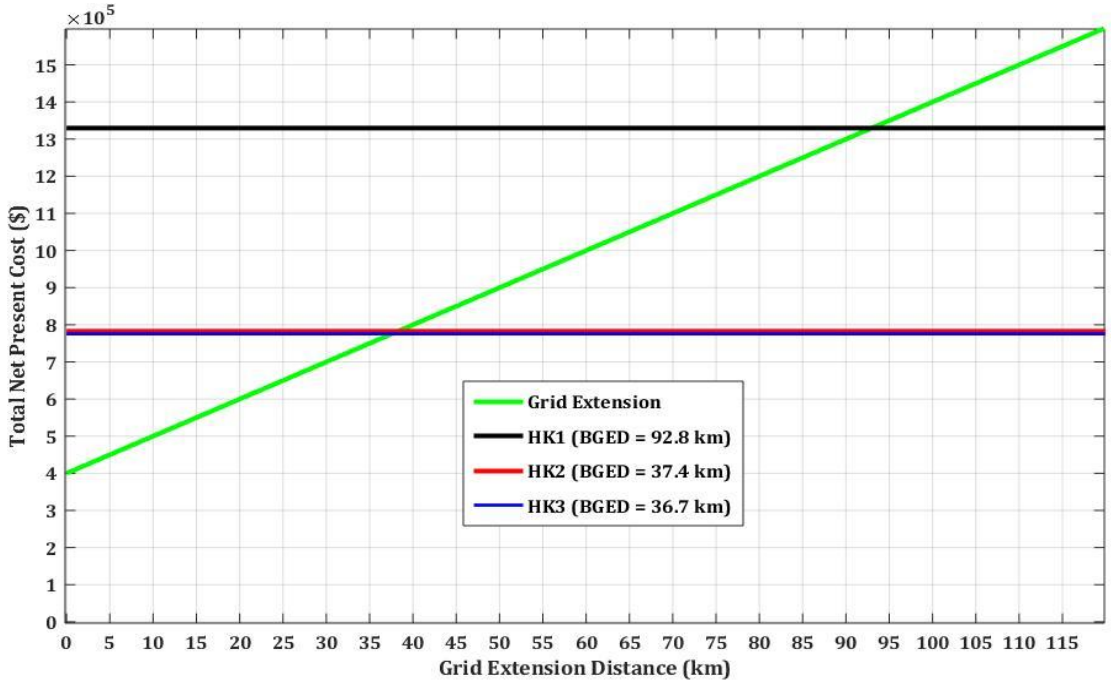

Figure 17: The breakeven distance for grid extension. The point of intersection between the grid extension line and the HESs gives the breakeven distance for subsequent HES.

5.2 Comparison with other studies

As discussed in the introduction, most HES simulations were performed for a single year disregarding the inevitable load growth. This study has employed the MYLG model, which allows explicit modelling of HESs for 25 years with increasing load over its lifetime. Hence the technical correlation between this study and most studies [14], [17]–[20] will be experienced during the first year only, with significant changes over its lifetime.

During the first year of the proposed HESs, both the solar radiation and hydrokinetic resources are the most significant energy producers with little contribution from the diesel generators. During the raining seasons (June-August) in the first year, over 90% of the load requirement was met from the HKTs production with an insignificant contribution from both the PV and Di-Gs. This observation is in correlation with previous studies [14], [17], [19] which concluded that hydropower resources would have the highest dispatch priority during high flow rate periods, being one of the most cost-competitive energy sources. These observations only depict a single year simulation; hence, different observations will be experienced as load demand increase over the years. During the last year of the project (25th year), the Di-G production was significant, up to 70% during the dry and 20% in the raining season despite the constant energy production from the HKTs. These results are similar to observations from [15], [16] which was experienced due to increment in the baseload of the system been met by the Di-Gs to avoid capacity shortage. The economics analysis from previous studies show COE ranging from $0.2-1.2/kWh [17], [18], [20] for HESs without hydropower resource while lower COE was achieved (0.06 – 0.4/kWh) for HESs with hydropower resource [14], [17], [19]. These results are in accordance with the results of $0.199 – 0.336/kWh obtained during the optimisation simulation of the proposed HESs.

The optimisation technique developed achieved the non-MYLG and MYLG discrepancies of 6.3%, 10.5%, and 11.2% for HK1, HK2 and HK3 respectively. A drop in discrepancy compared to 17.5% obtained by [16]. The result also shows that the lower the sequential scaling employed, the lower the value of discrepancies, but with longer duration for simulations. Therefore, the pre-optimisation technique developed for MYLG can be employed in further studies to obtain homogenous techno-economic results between non-MYLG and MYLG.

5.3 Emissions

Table 9. shows all the pollutant from the system, calculated base on the emission factor and annual diesel consumption. The most significant emitted compound is carbon dioxide (CO_2), which has received debate from environmentalists [1], [3], [6]. The HK2 scenario has the highest CO_2 emission; hence, it is considered as the least environmentally friendly of all the scenarios simulated. The CO_2 emitted can be compared with emission from the grid electricity using the grid emission factor in Nigeria (0.440 $kgCO_2eq/kWh$) [39]. The load served by HK2 during the first year was (244,859 kWh) and (497,748 kWh) in the last year. If this amount of energy were to be supplied by the grid electricity, the emission would be 107,737 kg and 219,009 kg for the first and last year, respectively. Therefore, the carbon saving from the HK2 for the first year was 62,158 kg (58%) and 30766 (14%) in the last year and an aggregate of 1280000 kg CO_2 savings through its lifetime. Even though HK2 has the highest emission from the HESs, it achieves a lower emission compared to the grid electricity in Nigeria. Therefore, all HESs will emit less pollutant compared to electricity production in Nigeria.

Table 9.
The emissions from the HESs. HK2 has the highest emission, consider as the least environmentally friendly but achieved a lesser emission compared to grid electricity.

		Emission (kg/year)					
	Emission factor	HK1		HK2		HK3	
	(g/L fuel)	1st year	25 year	1st year	25 year	1st year	25 year
CO_2	**	42,375	199,195	45,579	188,243	27,119	134,156
CO	16.34	265	1,295	285	1,229	169	873
UHC	0.72	11.7	54.8	12.5	51.8	7.46	36.9
PM	0.098	1.58	6.52	1.69	6.06	1.01	4.37
SO_2	0.65	104	488	112	461	66.4	329
NO_x	1.5359	246	681	260	590	157	446

** - Calculated from the properties of diesel: Carbon content of diesel(88%),
Lower Heating Value of Diesel (43.2MJ/kg) & Density of diesel (820 kg/m3) [21]
CO - Carbon monoxide; UHC - Unburned hydrocarbons; PM - Particulate matter;
SO_2 - Sulfur dioxide; NOx - Nitrogen oxides

5.4 Limitations and the impact of government policies

Sales of energy is the major limitation against the profitability of MGs for private organisations. The cheapest COE ($0.2/kWh) from the HESs were not cost-competitive with the current COE $0.1/kWh [37] from the grid in Nigeria. Additionally, the target community are predominantly fishermen and farmers with low yearly income index of $120 per capita [40]. Hence, the price of electricity even at the grid level might not be affordable to the villagers.

Interestingly, a study by Alam and Bhattacharyya (2017) [41] found that the rural dwellers of a developing country (Bangladesh) have willingness-to-pay (WTP) up to $0.432/kWh for the introduction of electricity into their community. This result shows the eagerness of rural dweller towards the introduction of electricity considering the socio-economic improvement. However, this value (WTP = $0.432/kWh) is infeasible for a household with an average daily income of $120 per capita in Nigeria [40]. Hence, favourable Government supports, policies and regulations toward MGs are essential in reducing energy poverty in rural areas.

Unfortunately, there are no Government policies towards HESs development in Nigeria. Although, the Renewable Energy Master Plan (REMP) developed by the Nigerian government was aimed at supporting RE technology. This initiative outlined the financial tools and incentives to be employed in other to increase the energy contribution from RE to 10% by 2025. REMP is currently inactive because it has not been signed into law [42]. However, 100% initial capital cost subsidy from the Government towards the proposed HESs will reduce the COE of HK2 and HK3 scenarios up to 50%, enough to achieve grid parity. Besides, the social responsibility of the government to provide public utilities such as jobs and improvement in the quality of life of her citizens are derivable from the proposed HESs. Hence, it is reasonable and economically cheaper for the Government to support the proposed HESs rather than GE.

6. Conclusion

The main objective of this study is to present a techno-economic and sensitivity analyses for cost-effective HESs incorporated with the MYLG functionality, aimed at providing electricity, and desalinated water for a rural community. In addition, to reduce the difference between the MYLG and non-MYLG results. Three design scenarios were considered based on the number(s) of HKT used (HK1- one HKT; HK2 – two HKT; turbines and HK3 – three HKT) in the HES consisting of PVs, BT, 50 and 100 kVA diesel generators.

The simulation was performed in HOMER software using two DAs (CC and LF) with the MYLG model set to 3%. The HKTs produced the most significant proportion of the energy throughout the project lifetime. The sensitivity analysis result shows that the increase in water speed will reduce the total NPC and COE because HK resources offer the cheapest source of energy for the rural location. The resulting configuration of Gen50/Gen100/PV/BT/HK was able to meet the growing load demand for all the 25 years simulated with 0% unmet load and capacity shortage; hence, the development of HES is a viable option towards the electrification of rural communities. The HK2 and HK3 provided the cheapest COE of $0.2/kWh relatively lower compared to previous studies but doubled the COE from the grid ($0.1/kWh). However, the life cycle cost assessment of the HESs are significantly cheaper than grid extension due to long-distance. Hence, the HESs are the most suitable for the location. The COE from the HESs will reduce significantly with support from the Governments in term of funding and policy.

Additionally, to obtain a homogenous economic result between the MYLG and non-MYLG, this study has introduced a novel technique of optimising MYLG through pre-optimisation of the non-MYLG and then sequentially scaling of the resulting capacities. With this method, the discrepancy between the non-MYLG and MYLG achieved 6.3% for HK1, 10.5% and 11.7% for HK2 and HK3 design scenarios respectively. This result shows that lower discrepancies could be achieved if lower sequential scaling is employed. Hence, this method can be employed in further study of

MYLG. Further research can be conducted to investigate the possible effect of predictive/probability DAs programmed in MATLAB with the application of lower sequential scaling and load sensitivity analyses.

Acknowledgements

The author wishes to thank Dr Jonathan Swingler for his fantastic supervision, reviews, and advice during the research. Also, further thanks to Dr Kocher Gudrun and Dr Wolf Fruh for their detailed reviews during the research.

Reference

[1] D. Tan, 'Energy Challenge, Power Electronics & Systems (PEAS) Technology and Grid Modernization', *IEEE CPSS Trans. Power Electron. Appl.*, vol. 2, no. 1, pp. 3–11, 2017.

[2] O. Rosnes and H. Vennemo, 'The cost of providing electricity to Africa', *Energy Econ.*, vol. 34, no. 5, pp. 1318–1328, 2012.

[3] E. Panos, M. Densing, and K. Volkart, 'Access to electricity in the World Energy Council's global energy scenarios: An outlook for developing regions until 2030', *Energy Strateg. Rev.*, vol. 9, pp. 28–49, 2016.

[4] Z. Li, A. Siddiqi, L. D. Anadon, and V. Narayanamurti, 'Towards sustainability in water-energy nexus: Ocean energy for seawater desalination', *Renew. Sustain. Energy Rev.*, vol. 82, no. October 2017, pp. 3833–3847, 2018.

[5] F. M. Gatta *et al.*, 'Replacing Diesel Generators with Hybrid Renewable Power Plants: Giglio Smart Island Project', *IEEE Trans. Ind. Appl.*, vol. 55, no. 2, pp. 1083–1092, 2019.

[6] T. Mai *et al.*, 'Renewable electricity futures for the United States', *IEEE Trans. Sustain. Energy*, vol. 5, no. 2, pp. 372–378, 2014.

[7] T. S. Ustun, C. Ozansoy, and A. Zayegh, 'Recent developments in microgrids and example cases around the world - A review', *Renew. Sustain. Energy Rev.*, vol. 15, no. 8, pp. 4030–4041, 2011.

[8] C. Mathieson *et al.*, 'Increasing renewable penetration on islanded networks through active network management: a case study from Shetland', *IET Renew. Power Gener.*, vol. 9, no. 5, pp. 453–465, 2015.

[9] E. Alegria, T. Brown, E. Minear, and R. H. Lasseter, 'CERTS microgrid demonstration with large-scale energy storage and renewable generation', *IEEE Trans. Smart Grid*, vol. 5, no. 2, pp. 937–943, 2014.

[10] E. H. Kim, J. H. Kim, S. H. Kim, J. Choi, K. Y. Lee, and H. C. Kim, 'Impact analysis of wind farms in the jeju Island power system', *IEEE Syst. J.*, vol. 6, no. 1, pp. 134–139, 2012.

[11] B. J. Williamson *et al.*, 'A Self-Contained Subsea Platform for Acoustic Monitoring of the Environment Around Marine Renewable Energy Devices-Field Deployments at Wave and Tidal Energy Sites in Orkney, Scotland', *IEEE J. Ocean. Eng.*, vol. 41, no. 1, pp. 67–81, 2016.

[12] B. Mangu, S. Akshatha, D. Suryanarayana, and B. G. Fernandes, 'Grid-Connected PV-Wind-Battery-Based Multi-Input Transformer-Coupled Bidirectional DC-DC Converter for Household Applications', *IEEE J. Emerg. Sel. Top. Power Electron.*, vol. 4, no. 3, pp. 1086–1095, 2016.

[13] H. Louie, E. O'Grady, V. Van Acker, S. Szablya, N. P. Kumar, and R. Podmore, 'Rural Off-Grid Electricity Service in Sub-Saharan Africa [Technology Leaders]', *IEEE Electrif. Mag.*, vol. 3,

no. 1, pp. 7–15, 2015.

[14] R. Sen and S. C. Bhattacharyya, 'Off-grid electricity generation with renewable energy technologies in India: An application of HOMER', *Renew. Energy*, vol. 62, pp. 388–398, 2014.

[15] A. Kumar, A. R. Singh, Y. Deng, X. He, P. Kumar, and R. C. Bansal, 'Multiyear load growth based techno-financial evaluation of a microgrid for an academic institution', *IEEE Power Access*, vol. 6, pp. 37533–37555, 2018.

[16] A. S. Aziz, M. F. N. Tajuddin, M. R. Adzman, A. Azmi, and M. A. M. Ramli, 'Optimization and sensitivity analysis of standalone hybrid energy systems for rural electrification: A case study of Iraq', *Renew. Energy*, vol. 138, pp. 775–792, 2019.

[17] S. Bahramara, M. P. Moghaddam, and M. R. Haghifam, 'Optimal planning of hybrid renewable energy systems using HOMER: A review', *Renew. Sustain. Energy Rev.*, vol. 62, pp. 609–620.

[18] T. Adefarati, R. C. Bansal, and J. John Justo, 'Techno-economic analysis of a PV–wind–battery–diesel standalone power system in a remote area', *J. Eng.*, vol. 2017, no. 13, pp. 740–744, 2017.

[19] H. S. Das, C. W. Tan, A. H. M. Yatim, and K. Y. Lau, 'Feasibility analysis of hybrid photovoltaic/battery/fuel cell energy system for an indigenous residence in East Malaysia', *Renew. Sustain. Energy Rev.*, vol. 76, no. December 2016, pp. 1332–1347, 2017.

[20] M. Soshinskaya, W. H. J. Crijns-Graus, J. van der Meer, and J. M. Guerrero, 'Application of a microgrid with renewables for a water treatment plant', *Appl. Energy*, vol. 134, pp. 20–34, 2014.

[21] 'HOMER - Hybrid Renewable and Distributed Generation System Design Software'. [Online]. Available: https://www.homerenergy.com/. [Accessed: 09-Jul-2019].

[22] 'Akassa - Google Maps'. [Online]. Available: https://www.google.com/maps/place/Akassa,+Nigeria/@4.3285921,6.0518907,15z/data=!3m1!4b1!4m5!3m4!1s0x106bb5822d27d4d7:0xadf8ecb48d3b3ff1!8m2!3d4.3281867!4d6.0641127. [Accessed: 09-Aug-2019].

[23] D. Nwoko, I. Nwaogazie, and C. Dike, 'Modelling Velocity Distribution in 3-D for Nun River, Niger Delta Nigeria', *Br. J. Appl. Sci. Technol.*, vol. 20, no. 6, pp. 1–12, 2017.

[24] A. P. Kenneth and A. J. Tarilanyo, 'Developing sustainable power supply for rural communities in akassa of bayelsa state using photovoltaic system and battery', *Res. J. Appl. Sci. Eng. Technol.*, vol. 6, no. 4, pp. 545–550, 2013.

[25] O. Adeoye and C. Spataru, 'Modelling and forecasting hourly electricity demand in West African countries', *Appl. Energy*, vol. 242, no. November 2018, pp. 311–333, 2019.

[26] O. B. Akpor and M. Muchie, 'Challenges in meeting the MDGs: The Nigerian drinking water supply and distribution sector', *J. Environ. Sci. Technol.*, vol. 4, no. 5, pp. 480–489, 2011.

[27] C. Ghenai, A. Merabet, T. Salameh, and E. C. Pigem, 'Grid-tied and stand-alone hybrid solar power system for desalination plant', *Desalination*, vol. 435, no. October 2017, pp. 172–180, 2018.

[28] F. I. Ibitoye and A. Adenikinju, 'Future demand for electricity in Nigeria', *Appl. Energy*, vol. 84, no. 5, pp. 492–504, 2007.

[29] Federal Republic of Nigeria, 'Annual Abstract of Statistics , Federal Republic of Nigeria National Bureau of Statistics', *Annu. Abstr. Stat.* 2012.

[30] 'POWER Data Access Viewer'. [Online]. Available: https://power.larc.nasa.gov/data-access-viewer/. [Accessed: 09-Jul-2019].

[31] T. Khatib, A. Mohamed, and K. Sopian, 'A review of photovoltaic systems size optimization techniques', *Renew. Sustain. Energy Rev.*, vol. 22, pp. 454–465, 2013.

[32] P. Wais, 'A review of Weibull functions in wind sector', *Renew. Sustain. Energy Rev.*, vol. 70, pp. 1099–1107, 2017.

[33] A. J. Sangster, 'Solar Photovoltaics: Cost analysis series', *Green Energy Technol.*, vol. 194, no. 4, pp. 145–172, 2014.

[34] V. P. Sector, 'Renewable Energy Technologies: Cost Analysis Series - Hydropower', *Int. Renew. Energy Agency*, vol. 1, no. 3, pp. 92–138, 2012.

[35] K. Kusakana, 'Feasibility analysis of river off-grid hydrokinetic systems with pumped hydro storage in rural applications', *Energy Convers. Manag.*, vol. 96, pp. 352–362, 2015.

[36] Ruud Kempener (IRENA) and Eric Borden, 'Battery Storage for Renewables : Market Status and Technology Outlook', *Int. Renew. Energy Agency*, 2015.

[37] V. O. Oladokun and O. C. Asemota, 'Unit cost of electricity in Nigeria: A cost model for captive diesel powered generating system', *Renew. Sustain. Energy Rev.*, vol. 52, pp. 35–40, 2015.

[38] W. Arowolo, P. Blechinger, C. Cader, and Y. Perez, 'Seeking workable solutions to the electrification challenge in Nigeria: Minigrid, reverse auctions and institutional adaptation', *Energy Strateg. Rev.*, vol. 23, no. December 2018, pp. 114–141, 2019.

[39] K. E. Enongene, F. H. Abanda, I. J. J. Otene, S. I. Obi, and C. Okafor, 'The potential of solar photovoltaic systems for residential homes in Lagos city of Nigeria', *J. Environ. Manage.*, vol. 244, no. April, pp. 247–256, 2019.

[40] R. O. Babatunde and M. Qaim, 'Patterns of income diversification in rural Nigeria: Determinants and impacts', *Q. J. Int. Agric.*, vol. 48, no. 4, pp. 305–320, 2009.

[41] M. Alam and S. Bhattacharyya, 'Are the off-grid customers ready to pay for electricity from the decentralized renewable hybrid mini-grids? A study of willingness to pay in rural Bangladesh', *Energy*, vol. 139, no. 2017, pp. 433–446, 2017.

[42] C. G. Monyei, A. O. Adewumi, M. O. Obolo, and B. Sajou, 'Nigeria's energy poverty: Insights and implications for smart policies and framework towards a smart Nigeria electricity network', *Renew. Sustain. Energy Rev.*, vol. 81, no. February 2017, pp. 1582–1601, 2018.

Appendix 1

Location Expanded Map

Map of the research location and surrounding villages.

Appendix 2

Battery Modelling

$$P_G(t) = \eta_s(P_{PV} + P_{DG} + P_{HT})$$

$$P_T = \pm[P_G(t) - P_L(T)]$$

Where $P_G(t)$ the aggregate available power from all the components in the system; η_s is the overall system efficiency; P_{PV} – Solar PV power; P_{DG} – Diesel generator power and P_{HT} – Hydrokinetic power output.

During Charge:

$$SOC(t + \Delta t) = min\{SOC(t)(1 - \sigma) + \eta_{bat,c}(P_T)\Delta t, SOC_{max}\}$$

During discharge:

$$SOC(t + \Delta t) = \begin{cases} SOC(t)\,(1 - \sigma) & if \dfrac{P_T}{\eta_{bat,dc}} > P_{lim,bat}^{lim} \\ max\{SOC(t)(1 - \sigma) - (P_T/\eta_{bat,dc})\Delta t, SOC_{min}\} & if \dfrac{P_T}{\eta_{bat,dc}} \geq P_{lim,bat}^{lim} \end{cases}$$

Where $(t, \Delta t)$ – time and time step in hours; SOC_{max}, SOC_{min} – maximum and minimum allowable state of the battery; σ – self-discharge coefficient of the battery; η_{bat} – battery's efficiency; $\eta_{bat,c}$, $\eta_{bat,dc}$ – charging and discharging efficiency respectively; $P_{lim,bat}^{lim}$ – power discharge limit of the battery which depends on both operating current discharge limit and voltage as $P_{bat}^{lim} = I_{bat}^{lim} * V_{bat}$.

Appendix 3

Grid Extension Parameters

Capital cost ($/km)	8,000 [21]
O/M cost ($/year/km)	160 [21]
Grid power price ($0.1/ kWh)	0.1 [21]